POLITECNICO DI TORINO
Repository ISTITUZIONALE

Fuel cell electrified propulsion systems for long-haul heavy-duty trucks: present and future cost-oriented sizing

Original
Fuel cell electrified propulsion systems for long-haul heavy-duty trucks: present and future cost-oriented sizing / Anselma, P.G., Belingardi, G.. - In: APPLIED ENERGY. - ISSN 0306-2619. - 321:(2022), p. 119354. [10.1016/j.apenergy.2022.119354]

Availability:
This version is available at: 11583/2965667 since: 2022-06-02T21:38:04Z

Publisher:
Elsevier

Published
DOI:10.1016/j.apenergy.2022.119354

Terms of use:

This article is made available under terms and conditions as specified in the corresponding bibliographic description in the repository

Publisher copyright
Elsevier postprint/Author's Accepted Manuscript

© 2022. This manuscript version is made available under the CC-BY-NC-ND 4.0 license http://creativecommons.org/licenses/by-nc-nd/4.0/.The final authenticated version is available online at: http://dx.doi.org/10.1016/j.apenergy.2022.119354

(Article begins on next page)

25 June 2026

Fuel Cell Electrified Propulsion Systems for Long-haul Heavy-duty Trucks: Present and Future Cost-oriented Sizing

Pier Giuseppe Anselma,[a,b,*] Giovanni Belingardi[a,b]

[a]*Department of Mechanical and Aerospace Engineering (DIMEAS), Politecnico di Torino, Corso Duca degli Abruzzi 24, 10129 Torino, Italy*

[b]*Center for Automotive Research and Sustainable Mobility (CARS), Politecnico di Torino, Corso Duca degli Abruzzi 24, 10129 Torino, Italy*

***Abstract*—Fuel cell electrified propulsion may currently represent a promising option for long-haul heavy-duty trucks. However, appropriately sizing fuel cell electrified propulsion systems to fully exploit the economic potential of this technology when applied to heavy-duty trucks still represents an open research question. To overcome this drawback, a methodology to size the fuel cell electrified propulsion system for a heavy-duty truck to minimize its total cost of ownership as function of different present- and future-oriented cost scenarios is presented in this paper.**

Retained cost contributions include both the retail price and the hydrogen and electricity lifetime costs as evaluated by implementing an optimal energy management approach in diversified driving missions. Fuel cell electrified truck powertrain sizing layouts are compared with battery electric powertrain option, and the latter is suggested as more appealing in the present cost scenario. Nevertheless, thanks to reductions forecasted in 10 years and 30 years both in terms of component costs, hydrogen cost and electricity cost, rightsizing the fuel cell electrified truck propulsion system according to the proposed methodology allows demonstrating its economic viability compared with a battery electric powertrain layout.

***Index Terms*—Cost-oriented sizing, Fuel cell, Heavy-duty truck, Optimal control, Total cost of ownership**

I. Introduction

The evolution towards a sustainable transport system requires advancing several vehicle electrification technologies [1]. Indeed, pure electric powertrains are suggested as an effective solution for applications with limited propelling energy demand such as A-class passenger cars as example [2]. Nevertheless, when it comes to higher power and energy demand applications such as long-haul heavy-duty trucks, the viability of battery electric propulsion may be significantly restrained by the power-to-weight ratio of current 400V and 800V lithium-ion based energy storage systems [3]. Battery swapping approaches might potentially enable pure battery electric propulsion of long-haul heavy-duty trucks, yet their feasibility has currently been assessed specifically for public transportation only [4]. Dynamic wireless power transfer represents a further potential enabler in this framework, yet it demands radically reshaping the road infrastructure [5][6].

In the depicted framework, fuel cell electrified vehicles (FCEVs) that are propelled by means of both hydrogen and electricity from the grid may represent a viable option for lowering the overall CO2 emissions of the heavy-duty transport sector [7][8]. Hydrogen may indeed serve as a second energy source in FCEVs which exhibits rapid refueling capability. However, several technological limitations currently restrain the widespread diffusion of FCEVs in the heavy-duty transport sector, including as example the overall cost of a FCEV, the lack of an extensive hydrogen refueling infrastructure and safety issues related to hydrogen storage [9]. A hydrogen fueling infrastructure could be intelligently designed by assessing refueling habits [10][11], while dedicated fault diagnosis methods may find development for fuel cell systems [12][13]. On the other hand, reducing the overall cost of a FCEV requires dedicated design and sizing procedures at early stages of the vehicle development.

Several research works can be found in literature regarding sizing of fuel cell systems for passenger cars. Wu and Gao in 2006 considered a fuel cell stack coupled with a supercapacitor bank as the energy storage system for a passenger car and sized the system to reduce the overall vehicle cost [14]. Optimal sizing a FCEV powertrain by coupling a fuel cell with a supercapacitor was proposed in 2010 by Hegazy and Van Mierlo [15] and in 2016 by Feroldi and Carignano [16]. Considering electrified city buses, powertrain architectures embedding either fuel cell and battery [17] or fuel cell, battery and supercapacitor were sized [18]. In 2008, Bauman and Kazerani compared three different FCEV powertrain layouts including (1) fuel cell-battery, (2) fuel cell-ultra capacitor, and (3) fuel cell-battery-ultra capacitor. The FCEV architecture embedding fuel cell and battery was suggested being the less costly option [19]. Even neglecting the powertrain cost, similar hydrogen economy capability was suggested between a fuel cell-battery and a fuel-cell capacitor FCEV layout for a passenger car in [20]. Since similarity between a passenger car and a commercial vehicle may be assumed from the electrified powertrain operational point of view, a fuel cell-battery FCEV powertrain layout is thus retained in this work.

Focusing on cost-oriented sizing of fuel cell-battery FCEV

* Corresponding author e-mail: pier.anselma@polito.it

powertrain layouts for long-haul heavy-duty trucks, some limitations can be highlighted in current literature. For example, when the FCEV supervisory controller is based on a heuristic energy management approach (e.g. inherited from Advisor), the optimality of the estimated hydrogen economy capability for a given powertrain design option is not guaranteed [21][22]. In other studies, only one standard drive cycle and one cost scenario are retained for sizing the heavy-duty truck fuel cell electrified powertrain, while neglecting the impact of various driving conditions and changing prices on the identification of the best design option [23]. Finally, few studies present sizing methodologies focused on specific powertrain components for the heavy-duty truck (e.g. hydrogen tank), thus neglecting their influence on the design of the remaining FCEV sub-systems [24][25].

To overcome the reviewed limitations of current design methodologies for sizing the fuel cell and the battery pack of an electrified long-haul heavy-duty truck, this paper aims at presenting a dedicated procedure. Hydrogen and electrical energy economy capabilities are evaluated in various driving conditions using a global optimal off-line FCEV control strategy. The sizing objective involves minimizing the total cost of ownership (TCO) of the fuel cell electrified long-haul heavy-duty truck including both retail price, lifetime hydrogen cost and lifetime electricity cost. Different cost scenarios are analyzed considering both 2020, 2030 and 2050 oriented possibilities. Results demonstrate that different costs for both FCEV powertrain components, hydrogen and electricity remarkably impact the best design option suggested by the proposed design methodology. The rest of this paper is organized as follows: the FCEV numerical model and the implemented energy management are presented first. The following section introduces the proposed cost-oriented FCEV propulsion system sizing methodology. Cost scenario-based FCEV sizing results for the long-haul heavy-duty truck are then discussed, and conclusions are finally drawn.

II. FCEV Model and Energy Management

This section aims at describing the approaches for numerically modeling and optimally controlling the fuel cell electrified long-haul heavy-duty truck powertrain. All the procedures described here are implemented in MATLAB® environment.

A. FCEV numerical model

Fig. 1 illustrates the considered fuel cell electrified long-haul heavy-duty truck powertrain layout, while TABLE I reports the retained vehicle and powertrain parameters. On the propulsion side, an electric motor/generator (EM) is linked to the heavy-duty truck chassis through a direct drive transmission, a differential, and the wheels of the driven axle. The energy storage and generation side includes the high-voltage battery pack, the fuel cell system and the hydrogen tank. The high-voltage battery pack may work as an energy buffer, or as a primary power source as well when appropriately upsized. In this work, the battery pack is assumed capable of being charged from the grid, thus achieving plug-in electrified truck operation.

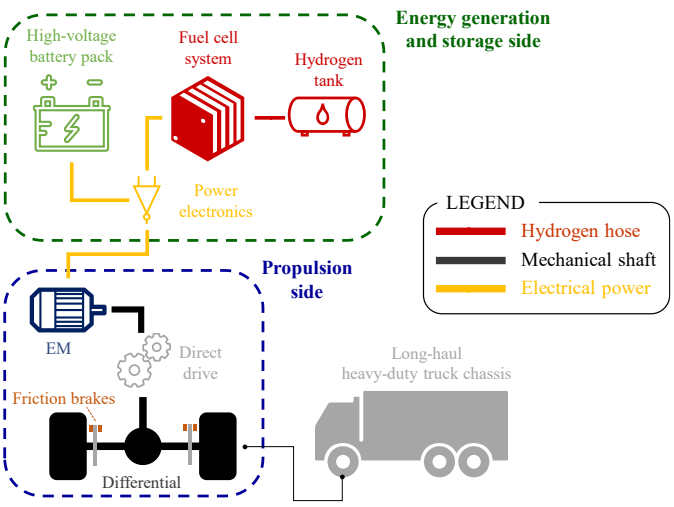

Fig. 1. Fuel cell electrified long-haul heavy-duty truck layout.

TABLE I
ELECTRIFIED HEAVY-DUTY TRUCK PARAMETERS

System	Symbol	Parameter	Value	Source
Vehicle body	r_{dyn}	Wheel dynamic radius	0.492 m	[27]
	c_r	Rolling friction coefficient	0.006	[27]
	c_d	Aerodynamic drag coefficient	0.73	[27]
	A_f	Frontal area	9.75 m^2	[27]
	ρ_{air}	Air density	1.225 kg/m^3	[27]
	g	Gravitational acceleration	9.81 m/s^2	[27]
Drive-line	η_{diff}	Differential efficiency	0.97	[27]
	η_{drive}	Direct drive efficiency	0.985^2	[27]
	τ_{tot}	EM to wheels gear ratio	7.5	[27]
EM	-	Type	PMSM	[27]
	-	Maximum power	391 kW	[27], [28]
	-	Maximum torque	2933 Nm	[27], [28]
Battery pack	Ah_{cell}	Cell capacity	41 Ah	[27]
	OCV_{nom}	Cell nominal voltage	3.62 V	[27]
	$n_{b,s}$	Number of cells in series	150	[27]
	$I_{cell_{min}}$	Maximum cell charge current	-150 A	[27]
	$I_{cell_{MAX}}$	Maximum cell discharge current	150 A	[27]
	SOC_{min}	Minimum cell SOC	8%	[27]
	SOC_{MAX}	Maximum cell SOC	89%	[27]
	P_{aux}	Electrical power of auxiliaries	4860 W	[27]
Fuel cell system	A_{cell}	Cell active area	200 cm^2	[20]
	$P_{cell_{MAX}}$	Maximum net power	0.477 W/cm^2	[20]
	$n_{FC,s}$	Number of cells in series	700	-
	LHV_{H_2}	Hydrogen lower heating value	141.8 kJ/g	[29]

Fuel cell system, high-voltage battery pack and EM are linked by means of power electronics, e.g. converters. A proton exchange membrane (PEM) fuel cell system is considered here.

The FCEV is modelled here following a quasi-static approach in deriving the battery electrical power and the fuel cell power from the requirements of the given driving mission while neglecting higher-order dynamic phenomena [26]. In this framework, the torque that the driveline is required to either

deliver or absorb at the driven wheels T_{wheels} can be evaluated in (1):

$$T_{wheels} = \left\{ m_{veh} \cdot [c_r \cdot g \cdot cos(\theta) + g \cdot sin(\theta) + a] + \frac{\rho_{air} \cdot A_f \cdot c_d \cdot v^2}{2} \right\} \cdot r_{dyn} \quad (1)$$

where m_{veh} represents the overall heavy-duty truck mass which is computed here as the sum of the different weight contributions. Further details regarding this procedure will be provided in the next section. v, a and θ stand for instantaneous values of vehicle speed, required vehicle acceleration and road slope, respectively, as provided by the driving mission requirements. The other parameters in (1) refers to TABLE I.

Then, angular speed ω_{EM} and torque T_{EM} of the EM can be evaluated as in eq. (2) and eq. (3), respectively:

$$\omega_{EM} = \frac{v}{r_{dyn}} \cdot \tau_{tot} \quad (2)$$

$$T_{EM} = \frac{T_{wheels} + T_{brake}}{\tau_{tot} \cdot (\eta_{diff} \cdot \eta_{drive})^{sign(T_{wheels})}} \quad (3)$$

where T_{brake} is the torque provided at the wheels by the friction brakes, while the remaining parameters are reported in TABLE I. τ_{tot} accounts for the gear ratios of both differential and direct drive, while including the sign of T_{wheels} as the exponential of the transmission efficiencies allows considering both propelling and braking cases.

The electrical power balance equation at the level of power electronics can be written as follows:

$$P_{FC} + P_{batt} = \omega_{EM} \cdot T_{EM} + \Lambda(\omega_{EM}, T_{EM}, SOC) + P_{aux} \quad (4)$$

where P_{FC} and P_{batt} denote the values of electrical power of the fuel cell system and the battery pack, respectively. Λ is the total electrical loss of the EM in watts, which can be evaluated by interpolating in a three-dimensional empirical table with torque, speed, and voltage of the EM as independent variables. The voltage of the EM in turn depends on the battery SOC, as it will be explained in the following equation. In this paper, a permanent magnet synchronous machine (PMSM) is considered and related values of maximum power and torque have been retained from [27], where a sizing procedure has been performed for the EM and the direct drive transmission to be embedded in the same heavy-duty truck considered here. The EM operational lookup table has been generated using the dedicated tool available in Amesim® software and following the methodology illustrated in [28]. P_{aux} represents the power consumption of the auxiliaries, i.e. air conditioning, electronic control unit, cooling circuit, electro-hydraulic power steering and electric air compressor [27].

Based on P_{batt}, the current of the battery pack I_{batt} can be evaluated according to an equivalent circuit model using (4):

$$I_{batt} = \frac{2 \cdot P_{batt}}{\sqrt{OCV(SOC) \cdot n_{b,s} - 4 \cdot P_{batt} \cdot R_{IN}(SOC) \cdot \frac{n_{b,s}}{n_{b,p}}} + OCV(SOC) \cdot n_{b,s}} \quad (4)$$

where OCV and R_{IN} respectively denote the open-circuit voltage and the internal resistance of a single cell of the battery pack. Both these variables can be determined by interpolating in a corresponding empirical one-dimensional lookup table with battery state-of-charge (SOC) as independent variables. Lookup tables considered here are retained from [27] accounting for different R_{IN} trends depending on charging or discharging events. $n_{b,s}$ and $n_{b,p}$ stand for the number of cells in series and in parallel, respectively, as per the battery pack configuration. $n_{b,s}$ is kept fixed to 150 in order to preserve the same battery pack nominal voltage of 520V, while $n_{b,p}$ represents a sizing variable as it will be discussed in the next section. Finally, the battery pack SOC at the generic time instant t can be evaluated by integrating I_{batt} over time as in eq. (5):

$$SOC(t) = SOC_0 - \int_0^t \frac{I_{batt}(t)}{Ah_{cell} \cdot 3600 \cdot n_{b,p}} dt \quad (5)$$

where Ah_{cell} and SOC_0 represent the cell capacity in ampere-hours and the battery SOC at the beginning of the driving mission, respectively.

When it comes to the fuel cell system, the hydrogen consumption rate in grams per second $\dot{H}_2$ can be evaluated as in eq. (6):

$$\dot{H}_2 = \frac{P_{FC}}{\eta_{FC}\left(\frac{P_{FC}}{A_{cell} \cdot n_{FC,s} \cdot n_{FC,p}}\right) \cdot LHV_{H_2}} \quad (6)$$

where η_{FC} is the efficiency of the fuel cell system which can be evaluated as a function of P_{FC}. Here, η_{FC} already considers the parasitic power of the auxiliary components of the fuel cell system (e.g. air compressor) [20]. Also in this case the number of cells in series $n_{FC,s}$ has been kept constant, while the number of cells in parallel $n_{FC,p}$ for the fuel cell system represents a sizing variable. Remaining parameters have been reported in TABLE I.

B. Optimal FCEV energy management

Predicting the hydrogen and battery energy economy of a given powertrain design candidate needs solving the optimal FCEV control problem in the considered driving missions [30]. The optimal FCEV control problem requires in turn minimizing the overall hydrogen consumption from the initial time instant to the final time instant t_{end} of the given driving mission while complying with considered constraints as illustrated in eq. (7) to eq. (10).

$$\arg\min \left\{ \int_0^{t_{end}} \dot{H}_2(t, P_{FC})\, dt \right\} \quad (7)$$

subject to:

Driveline constraints:

$$\begin{gathered} T_{EM}(t) = f[v(t), a(t), \theta(t), T_{brake}(t)] \\ T_{EM_{min}}[\omega_{EM}(t)] \leq T_{EM}(t) \\ T_{EM}[t, v(t) < v_{cut-off}, T_{wheels}(t) < 0] = 0 \end{gathered} \quad (8)$$

Battery pack constraints:

$$\begin{gathered} SOC(t_{end}) \geq SOC_{lim} \\ I_{batt}(t) = g[SOC(t), \omega_{EM}(t), T_{EM}(t), P_{FC}(t)] \\ SOC_{min} \leq SOC(t) \leq SOC_{MAX} \\ I_{cell_{min}} \cdot n_{b,p} \leq I_{batt}(t) \leq I_{cell_{MAX}} \cdot n_{b,p} \end{gathered} \quad (9)$$

Fuel cell system constraints:

$$0 \le P_{FC}(t) \le P_{cell_{MAX}} \cdot A_{cell} \cdot n_{FC,s} \cdot n_{FC,p}$$
$$\dot{P}_{FC_{min}} \le \dot{P}_{FC}(t) \le \dot{P}_{FC_{MAX}} \quad (10)$$

The driveline constraints reported in eq. (8) involve complying with the driving mission speed and road slope profiles over time while limiting the regenerative electrical power within the physical limitations of the EM. The eventual requirement of a more aggressive deceleration involves the intervention of friction brakes to supply the extra torque required to brake the truck. Moreover, regenerative braking is disabled below a certain vehicle speed value $v_{cut-off}$ which is set here to 10km/h [31]. Concerning battery pack constraints reported in (9), the SOC at the end of the given driving mission should not fall below a certain threshold SOC_{lim}, set here to 11% as per the cell specifications. Moreover, instantaneous values of both battery SOC and current need to be limited within allowed limits. Moving to the fuel cell system constraints reported in (10), its power is limited within physically allowed values as well. Furthermore, the instantaneous change in fuel cell power ($\dot{P}_{FC}$) is constrained within corresponding limits $\dot{P}_{FC_{min}}$ and $\dot{P}_{FC_{MAX}}$ in order to account for fuel cell dynamics that are mainly related to the slow dynamic of the air circuit [32]. In this paper, $\dot{P}_{FC_{min}}$ and $\dot{P}_{FC_{MAX}}$ are respectively set to -30% and +10% of the fuel cell system maximum power per second [33].

Dynamic programming (DP) is implemented here as a popular technique to effectively solve the illustrated FCEV optimal control problem [34][35]. DP represents an energy management approach that is widely implemented in electrified powertrain design methodologies thanks to its capability of automatically evaluating the ideal energy economy for a given sizing candidate in retained driving missions [36][37]. As an off-line method, DP requires the a priori knowledge of the entire driving mission beforehand [38]. Then, the global optimal solution for the considered dynamic control problem is identified by exhaustively sweeping at each time instant all the possible values of control and state variables [39]. The control variable set U_{DP} and state variable set X_{DP} considered in this work are reported in eq. (11).

$$U_{DP} = \{\dot{P}_{FC}\} \;\; ; \;\; X_{DP} = \begin{Bmatrix} P_{FC} \\ SOC \end{Bmatrix} \quad (11)$$

The control variable set includes the rate of fuel cell power and its discretization step is set to 5% of the fuel cell system maximum power as a reasonable trade-off between accuracy and grid size. Indeed, enlarging the discretization step for the fuel cell power above 5% of the fuel cell system maximum power has been observed slightly worsening the predicted hydrogen economy capability. On the other hand, reducing the discretization step for the fuel cell power below 5% of the fuel cell system maximum power has been found significantly increasing the computational cost required by DP without further improving the value of predicted hydrogen economy.

X_{DP} includes those variables whose evolution needs tracking over time throughout the driving mission. Battery SOC is retained both for evaluating at each time instant open-circuit voltage and internal resistance of the battery, and for ensuring compliance with corresponding optimal control constraints.

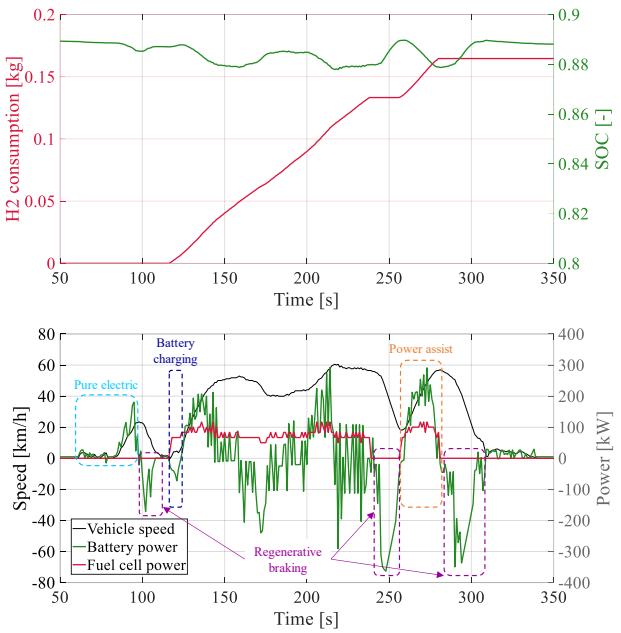

Fig. 2. Time series of cumulated hydrogen consumption, battery SOC, fuel cell power and battery power predicted by DP over a selected portion of CSHVR for the electrified heavy-duty truck embedding a 334kW fuel cell system and an 86kWh battery pack.

The fuel cell system power is considered and updated at each time instant based on the controlled value of $\dot{P}_{FC}$. The cost function that needs minimization within the DP algorithm J_{DP} for the overall driving mission can thus be evaluated in eq. (12):

$$J_{DP} = \int_0^{t_{end}} \left\{ \dot{H}_2 \left[t, \left(\int_0^t \dot{P}_{FC}(t)dt \right) \right] + \lambda_{act} \cdot \mu_{FC,act} \right\} dt \quad (12)$$

where the hydrogen consumption over time depends on the fuel cell system power which can be obtained by integrating $\dot{P}_{FC}$ while assuming that the fuel cell system is at rest in the first time instant. The second term in J_{DP} aims at avoiding frequent fuel cell system de/activations, and it involves λ_{act} as a constant weighting factor and $\mu_{FC,act}$ as a binary flag detecting fuel cell system activation based on instantaneous values of control and state variables.

A generic DP MATLAB® toolbox has been used in this work made available from Sundstrom and Guzzella [40]. Since the retained DP tool allows constraining final values of state variables, the fuel cell system power and the battery SOC have been set to be 0 and greater than SOC_{lim} at the end of each retained driving mission, respectively [41]. As example, Fig. 2 illustrates results obtained using the described DP in a selected portion of City Suburban Heavy Vehicle Cycle & Route (CSHVR) for the electrified heavy-duty truck embedding a 334kW fuel cell system and an 86kWh battery pack.

It should be admitted that, due to both its offline nature and its computational cost, DP may not straightforwardly be implemented as on-board control strategy in a FCEV. Nevertheless, a broad and ongoing research topic aims at developing FCEV real-time capable energy management systems that can achieve optimal performance in terms of hydrogen saving comparable with corresponding performance achieved by DP [42][43]. DP itself may serve in these processes as the reference benchmark for real-time controllers under

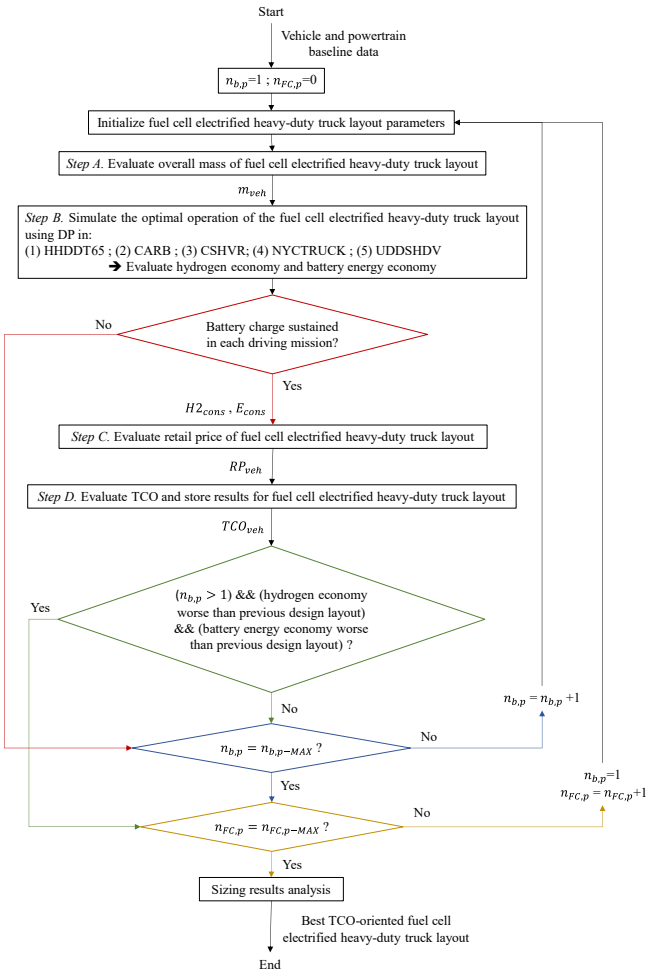

Fig. 3. Flowchart of the cost-oriented sizing methodology for fuel cell electrified propulsion systems of long-haul heavy-duty trucks.

development [44][45].

III. Cost-oriented FCEV Propulsion System Sizing

On the basis of the presented approaches for modeling a fuel cell electrified heavy-duty truck and for predicting its optimal energy economy capability, this section aims at introducing the TCO-oriented sizing procedure for the related fuel cell electrified powertrain. Looking at Fig. 1, the propulsion side of the FCEV powertrain can be sized in terms of gear ratios and EM aiming at complying with vehicle drivability requirements and at minimizing the EM electrical loss while simulating predefined driving missions. For the sake of conciseness, in this paper the propulsion side of the FCEV powertrain is considered already sized based on the results presented in [27] for the same heavy-duty truck considered here that embeds a single EM and a direct drive transmission. On the other hand, the energy storage and generation side of the FCEV propulsions system in Fig. 1 is the focus of the sizing methodology discussed here. The number of fuel cell branches in parallel $n_{FC,p}$ and the number of battery branches in parallel $n_{b,p}$ particularly represent the two sizing parameters that, in our aim, require determination. Fig. 3 illustrates the overall workflow of the related cost-oriented sizing methodology. Vehicle and powertrain baseline data are retained, and the parameters corresponding to the fuel cell heavy-duty truck layout under analysis are initialized. Battery pack capacity and fuel cell system power are particularly set based on selected values of $n_{FC,p}$ and $n_{b,p}$. $n_{FC,p}$ and $n_{b,p}$ are respectively set to 0 (i.e. battery electric powertrain layout) and 1 in the first iteration of the sizing algorithm.

TABLE II
Electrified Heavy-duty Truck Mass Contributions

System	Symbol	Parameter	Value	Source
Vehicle body	m_{tr}	Tractor mass	5,400 kg	[27]
	m_{tl}	Trailer mass	7,500 kg	[27]
	m_{ca}	Cargo mass	25,000 kg	[27]
Drive-line	m_{gb}	Transmission mass	139 kg	[27]
EM	m_{EM}	Electric motor mass	312 kg	[27]
	m_{in}	Inverter mass	39 kg	[27]
Battery pack	m_b	Battery pack mass	Proportional to $n_{b,p}$ as in (14)	[27]
Fuel cell system	m_{FC}	Fuel cell system mass	Proportional to $n_{FC,p}$ as in (15)	[20]
	m_{ta}	Hydrogen storage system mass	544 kg	[46], [47]

A. Vehicle mass determination

Step A in Fig. 3 involves determining the overall truck mass m_{veh} based on the size of the components to be embedded in the given FCEV powertrain design candidate. To this end, m_{veh} can be evaluated in (13) as the sum of various contributions:

$$m_{veh} = m_{tr} + m_{tl} + m_{ca} + m_b + m_{in} + m_{EM} + m_{gb} + m_{FC} + m_{ta} \quad (13)$$

where m_{tr}, m_{tl} and m_{ca} represent the tractor mass, the trailer mass, and the cargo mass, respectively. m_b is the mass of the battery pack, while m_{in}, m_{EM} and m_{gb} respectively relate to mass contributions for inverter, EM and transmission. Finally, m_{FC} and m_{ta} stand for the masses of the fuel cell system and the hydrogen storage system, respectively. Values and related sources for the mass contributions considered here are reported in TABLE II. Concerning m_{ta}, its values has been evaluated considering the baseline 31 kg hydrogen storage capability of Hyunday Xcient® fuel cell truck [46] and retaining 5.7% gravimetric density as observed for Toyota Mirai® [47]. On their behalf, m_b and m_{FC} are evaluated in kilograms according to the number of fuel cell branches and battery cell branches in parallel for each FCEV powertrain layout candidate as in eq. (14) and eq. (15), respectively.

$$m_b = 6.7 \cdot \frac{Ah_{cell} \cdot n_{b,p} \cdot OCV_{nom} \cdot n_{b,s}}{1000} \quad (14)$$

$$m_{FC} = 3 \cdot \frac{P_{cell_{MAX}} \cdot A_{cell} \cdot n_{FC,s} \cdot n_{FC,p}}{1000} \quad (15)$$

Where the weighting coefficients 6.7kg/kWh and 3kg/kW for the battery pack mass and the fuel cell system mass have been retained from [27] and [20], respectively.

B. Hydrogen and electrical energy economy evaluation

Once the overall mass of the FCEV powertrain layout under analysis has been determined, its hydrogen and battery energy economy capability need determination at Step B in Fig. 3. For the sake of assessing various real-world driving conditions, five driving missions experimentally collected considering heavy-duty vehicles have been retained from ADVISOR including (1) Heavy Heavy-Duty Diesel Truck 65 (HHDDT65), (2) CARB Heavy Heavy-Duty Diesel Truck Composite Cycle (CARB), (3) CSHVR, (4) New York City Truck Driving Schedule (NYCTRUCK), and (5) Urban Dynamometer Driving Schedule for Heavy-Duty Vehicles (UDDSHDV) [48].

In 2019, Liimatainen et al. have estimated the maximum daily distance travelled by long-haul trucks to rarely exceed 400 kilometers, which is retained here as the distance to be covered without charging the high-voltage battery pack from the grid [49]. Each of the 5 driving missions listed above has therefore been considered steadily repeated until 400 km driven were achieved. The DP algorithm described in Section II.B is then applied to evaluate the hydrogen and electrical energy economy capabilities of the FCEV powertrain layout under analysis in each of the five considered driving missions. The battery is particularly assumed charged up to SOC_{MAX} when starting each driving mission. Then, both hydrogen consumption capability $H2_{cons}$ in kilograms per 100 kilometers and electrical energy consumption capability E_{cons} in kilowatt-hours per 100 kilometers for the retained FCEV powertrain design options are evaluated as the average of the single values related to the five driving missions. At this point, an initial check is conducted in Fig. 3 for the FCEV design candidate being able to avoid excessively depleting the battery energy in any of the retained driving missions. In case the FCEV layout option under analysis cannot comply with battery SOC limits set in at least one driving mission (e.g. due to insufficient fuel cell system power), this is discarded and the next candidate is examined. Alternatively, the workflow is continued.

C. Retail price evaluation

Step C in Fig. 3 relates to evaluating the retail price of the fuel cell heavy-duty truck design option under analysis RP_{veh} using eq. (16):

$$RP_{veh} = c_{ch} + c_{in} + c_{EM} + c_{gb} + \alpha_{FC} \cdot \left(\frac{P_{cell_{MAX}} \cdot A_{cell} \cdot n_{FC,s} \cdot n_{FC,p}}{1000}\right) + c_{ta} + \alpha_{ba} \cdot \left(\frac{Ah_{cell} \cdot OCV_{nom} \cdot n_{b,s} \cdot n_{b,p}}{1000}\right) \quad (16)$$

where c_{ch}, c_{in}, c_{EM}, and c_{gb} represent retail price contributions for the truck chassis (including body, wheels, and other components), the inverter, the EM and the transmission, respectively. Values for these parameters are retained from [27] and amount to 75,000€, 5,865€, 6,256€ and 2,323€, respectively. α_{FC} and α_{ba} stand for the retail price coefficients for the fuel cell system in euro per kilowatt and for the battery pack in euro per kilowatt-hour, respectively. Overall retail price for the fuel cell system and the battery pack can thus be evaluated by multiplying α_{FC} and α_{ba} by the fuel cell system maximum power and the battery pack capacity, respectively. Finally, c_{ta} represents the retail price for the hydrogen storage system. α_{FC}, α_{ba}, and c_{ta} are not fixed in this work, yet they are varied depending on the cost scenario considered, as it will be discussed in section IV.A.

D. TCO evaluation

Once the hydrogen economy, the electrical energy economy, and the retail price of the FCEV design layout under analysis have been evaluated in the two previous steps, step D in Fig. 3 aims at determining the related TCO (TCO_{veh}). This is achieved using eq. (17):

$$TCO_{veh} = RP_{veh} + \frac{[\alpha_{H2} \cdot H2_{cons} + \alpha_{elec} \cdot E_{cons}]}{100} \cdot d_{year} \cdot life_{veh} \quad (17)$$

where α_{H2} and α_{elec} represent the hydrogen cost and the electricity cost in euro per kilogram and euro per kilowatt-hour, respectively. Both these parameters depend here on the cost scenario considered. d_{year} is the distance covered yearly by the long-haul heavy-duty truck under design, and it is assumed here being 110,000 kilometers [50]. Finally, $life_{veh}$ represents the expected economic lifetime of the long-haul heavy-duty truck under design, which is assumed being 8 years here [27].

E. FCEV powertrain sizing space exploration

The TCO associated with the FCEV powertrain sizing candidate under analysis has been evaluated and stored in the previous steps. When selecting the next sizing option to be analyzed, a brute force algorithm is retained here to exhaustively explore the considered FCEV sizing space. Even though different algorithms may be implemented to improve the computationally efficiency of the sizing space exploration process (e.g. genetic algorithm, particle-swarm optimization), a brute force method allows thoroughly observing the impact of the cost scenario parameters on the various FCEV sizing options retained. The brute force algorithm for exploring the FCEV sizing space finds illustration in Fig. 3. It should be noted that, when progressively increasing the number of battery cells in parallel $n_{b,p}$, while increasing $n_{FC,p}$, in case the FCEV sizing candidate exhibits worsen performance both in terms of hydrogen consumption and electrical energy consumption compared with the previously analyzed sizing option, $n_{b,p}$ is set back to 1. This is performed in order to improve the computational efficiency of the overall sizing process by reducing the number of sizing candidates to be analyzed.

Once all sizing candidates have been considered, the workflow illustrated in Fig. 3 is concluded and the sizing results can be analyzed.

IV. Fuel Cell Electrified Heavy-Duty Truck Sizing Results

This section aims at presenting results obtained for the introduced FCEV powertrain sizing methodology. Retained present- and future-oriented cost scenarios are presented first, followed by the discussion of the sizing results.

A. Cost scenarios

Five FCEV cost parameters still need definition that were introduced in both sub-sections III.C and III.D. These relate to (1) the retail price coefficient for the fuel cell system α_{FC}, (2) the retail price coefficient for the battery pack α_{ba}, (3) the retail price for the hydrogen storage system c_{ta}, (4) the hydrogen cost α_{H2}, and (5) the electricity cost α_{elec}. For the sake of assessing

the best FCEV sizing candidate based on present- and future-oriented cost parameters, six different cost scenarios are considered in this paper by varying the abovementioned cost parameters. Table III reports the considered values for the five cost parameters as function of the six cost scenarios retained, along with the corresponding references. "2020" scenario considers current values for cost parameters, in particular the hydrogen cost of 7.44€/kg was determined in [52] by analyzing real-world refueling stations for buses. "2030" scenario has been defined according to current projections for both fuel cell system, battery pack, hydrogen storage system, hydrogen and electricity costs in ten years. As it can be seen in TABLE III, current 2030 projections assume significant reductions in all the cost parameters compared with "2020" scenario. Finally, four 2050-projected different cost scenarios are considered. These share the same cost parameters for fuel cell system, battery pack and hydrogen storage system. A further reduction in these three retail price parameters is currently forecasted compared with both "2020" and "2030" scenarios thanks to technological advances and a considerable amount of research and development activities. Operative cost parameters related to hydrogen and electricity might exhibit in thirty years higher variability and uncertainty linked to future energy policies and regulations worldwide. To mitigate this shortcoming, compared with "2030" scenario, the four 2050 scenarios can be generated by assuming either an increase in both electricity and hydrogen costs ("2050-H2high-Ehigh"), or a decrease in both electricity and hydrogen costs ("2050-H2low-Elow"), or a decrease in one cost contribution and an increase in the other one ("2050-H2lowEhigh" and "2050-H2highElow"). These fluctuations for both hydrogen and electricity prices are based here upon forecasted values found in consulted references. As example, different 30 year-oriented hydrogen price projections might stem from forecasting the cost associated to the electrolysis within the hydrogen production process, among other factors [58][59].

TABLE III
FCEV COST PARAMETERS ACROSS PRESENT AND FUTURE SCENARIOS

Cost scenario	α_{FC} [€/kW]	α_{H2} [€/kg]	c_{ta} [€]	α_{ba} [€/kWh]	α_{elec} [€/kWh]
2020	206 [51]	7.44 [52]	27,900 [53]	250 [27]	0.21 [54]
2030	49 [55]	1.93 [56]	17,422 [55]	80 [55]	0.11 [57]
2050-H2low-Elow	36 [55]	1.16 [58]	14,012 [55]	71 [55]	0.10 [57]
2050-H2high-Ehigh	36 [55]	2.80 [59]	14,012 [55]	71 [55]	0.17 [58]
2050-H2low-Ehigh	36 [55]	1.16 [58]	14,012 [55]	71 [55]	0.17 [58]
2050-H2high-Elow	36 [55]	2.80 [59]	14,012 [55]	71 [55]	0.10 [57]

B. Scenario-based FCEV Sizing Results

Before starting the FCEV powertrain sizing workflow illustrated in Fig. 3, maximum values for $n_{FC,p}$ and $n_{b,p}$ have been set to 9 and 51 in this paper, respectively. This leads to generate a sizing space comprising totally 510 candidates. Out of them, 136 candidates were found not achieving battery charge-sustenance, while 225 candidates were found worsening both hydrogen economy and electrical energy economy capabilities compared with the previously analyzed candidates. The remaining 149 candidates were assessed according to the implemented sizing methodology. On average, around 51 minutes are required to simulate the fuel cell electrified heavy-duty truck controlled by DP while travelling one of the five 300-kilometer-long driving missions retained using a desktop computer with Intel Core i7-8700 (3.2 GHz) and 32 GB of RAM. This leads to 51x5x149=37,995 minutes (i.e. around 23 days) being required to complete the presented overall FCEV powertrain sizing methodology. Obtained sizing results are illustrated in Fig. 4 in terms of vehicle TCO as function of fuel cell system power and battery pack capacity for all the retained cost scenarios. The best FCEV powertrain sizing option is shown as well in each scenario sub-plot in Fig. 4, while related design and performance parameters are reported in TABLE IV. Finally, Fig. 5 illustrates cost breakdown of the suggested heavy-duty truck powertrain layouts as a function of the considered cost scenarios.

In the present "2020" scenario, the implemented sizing methodology suggests that, from a TCO perspective, a battery electric heavy-duty truck powertrain layout may be more appealing than a fuel cell electrified propulsion system. Indeed, not embedding the fuel cell system allows removing the cost contributions related to fuel cell system production, hydrogen storage system production, and hydrogen consumption. The higher weighting factors for these cost contributions reported in TABLE III for the present "2020" scenario indeed entail higher costs for the fuel cell electrified powertrain layouts as it can be observed in Fig. 4(a). As a downside, remarkable upsizing the battery pack is needed to meet the 400-kilometer range requirement in pure electric operation. As reported in TABLE IV, the overall truck mass increases up to more than 46 ton mainly due to the required 1.1 MWh battery pack. On the other hand, significant reductions forecasted for values of α_{FC}, c_{ta}, and α_{H2} in the "2030" scenario compared with the present scenario corroborate the TCO viability of a fuel cell electrified truck powertrain layout in around ten years' time. In particular, the automated sizing methodology suggests a 334kW fuel cell system coupled with a downsized 87kWh battery pack as the best powertrain layout in the "2030" scenario as shown in Fig. 4(b). Reducing the overall weight by 12.5%, the retail price by 64.8%, the TCO by 59.4% might be achieved in this way for the long-haul heavy-duty truck in 2030 compared with 2020 through right-sizing the fuel cell electrified propulsion system as reported in TABLE IV and in Fig. 5.

Moving to the 2050 oriented cost scenario results, when the hydrogen price is forecasted to be as low as 1.16€/kg (i.e. "2050-H2low-Elow" and "2050-H2lowEhigh"), the implemented sizing methodology suggests as best option the same FCEV powertrain layout as for the "2030" scenario. In these assumed 2050 cost scenarios, hydrogen still seems a much more viable energy source for the electrified propulsion of long-

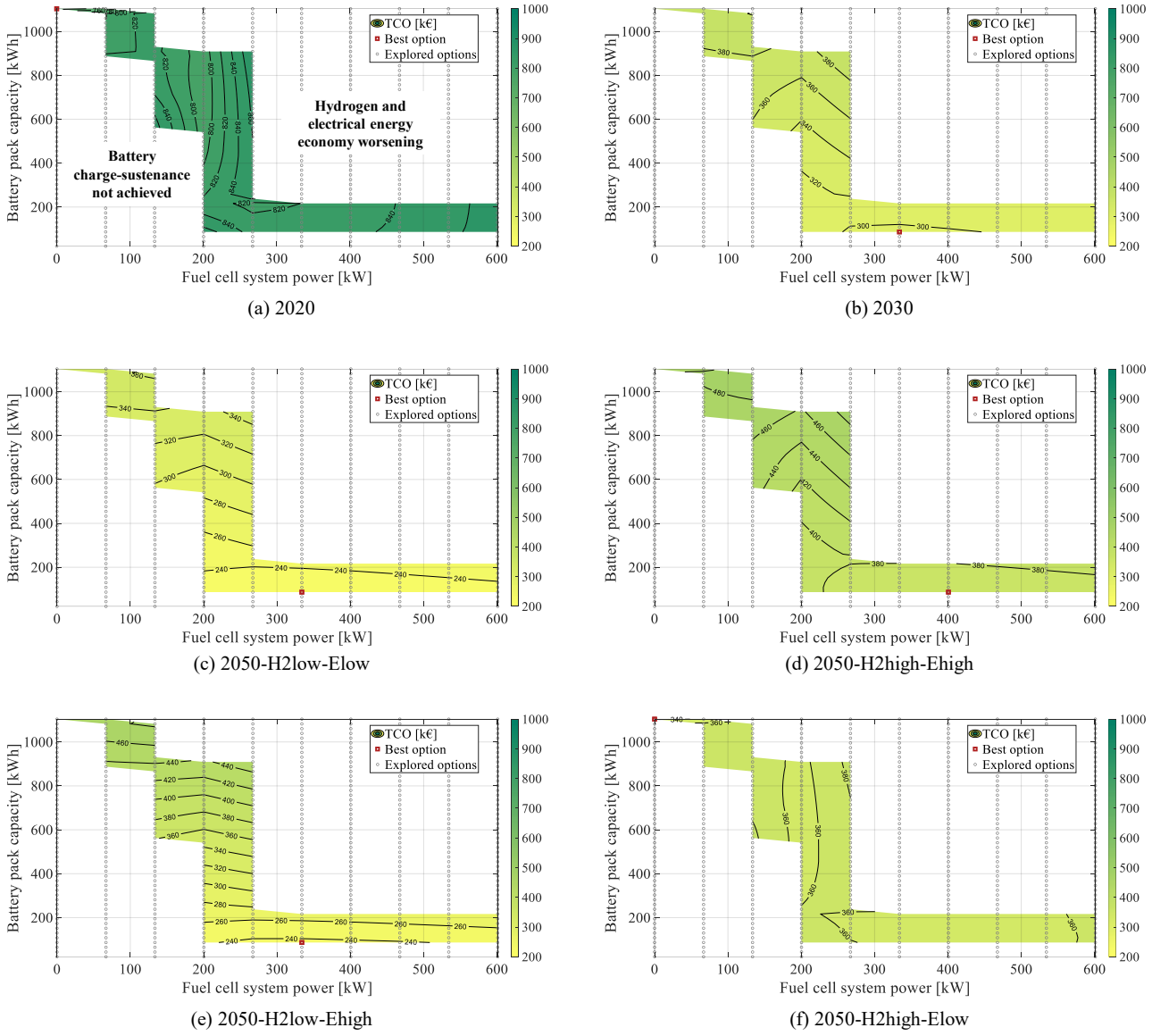

Fig. 4. FCEV TCO as function of fuel cell system power and battery pack capacity across retained cost scenarios.

haul heavy-duty trucks by means of fuel cell systems compared with electricity. Indeed, the sizing methodology chooses to remarkably downsize the battery pack which in turns serves as energy buffer rather than primary energy source for traction, entailing significant reductions both in terms of vehicle weight and retail price. As consequence, the electricity price fluctuation assumed between "2050-H2low-Elow" and "2050-H2lowEhigh" scenarios has a limited 1,000€ impact on the overall truck TCO, as it can be seen in Fig. 5 as well.

When an increase is assumed in 2050 for both hydrogen and electricity prices (i.e. "2050-H2high-Ehigh"), the implemented sizing methodology suggests to slightly increase the fuel cell system power by 67kW compared with the "2030" scenario. Such upsizing of the fuel cell system allows reducing the hydrogen consumption estimated using DP (e.g. through operating the fuel cell system in more efficient power regions) and in turn the hydrogen lifetime cost by around 1%. This reduction in the lifetime hydrogen cost is suggested capable of counterbalancing the increase in retail price due to the fuel cell system upsizing for the considered cost scenario. Finally, when an increase in the hydrogen price is forecasted along with a reduction in the electricity price (i.e. "2050-H2highElow"), the battery electric powertrain layout is again suggested to be more competitive compared to a fuel cell electrified propulsion system option.

C. Cost attractiveness of fuel cell electrified truck layouts versus pure electric truck layouts

Such diversified sizing results as a function of the considered cost scenario demand further investigation regarding the hydrogen price required for fuel cell electrified heavy-duty trucks to be more appealing than battery electric heavy-duty trucks. Results aiming at answering this research question are illustrated in Fig. 6, where the hydrogen price corresponding to the break-even point (BEP) between fuel cell truck and battery electric truck in terms of TCO has been plotted as a function of

TABLE IV
SUGGESTED FCEV POWERTRAIN DESIGN PARAMETERS ACROSS PRESENT AND FUTURE COST SCENARIOS

Cost scenario	Fuel cell system power [kW]	Battery pack capacity [kWh]	$H2_{cons}$ [kg/ 100 km]	E_{cons} [kWh/ 100 km]	m_{veh} [ton]	TCO_{veh} [k€]
2020	0	1104	0.0	196.1	46.3	731.3
2030	334	87	9.1	16.0	40.5	297.1
2050-H2low-Elow	334	87	9.1	16.0	40.5	225.8
2050-H2high-Ehigh	401	87	9.0	16.0	40.7	366.3
2050-H2low-Ehigh	334	87	9.1	16.0	40.5	235.7
2050-H2high-Elow	0	1104	0.0	196.1	46.3	338.0

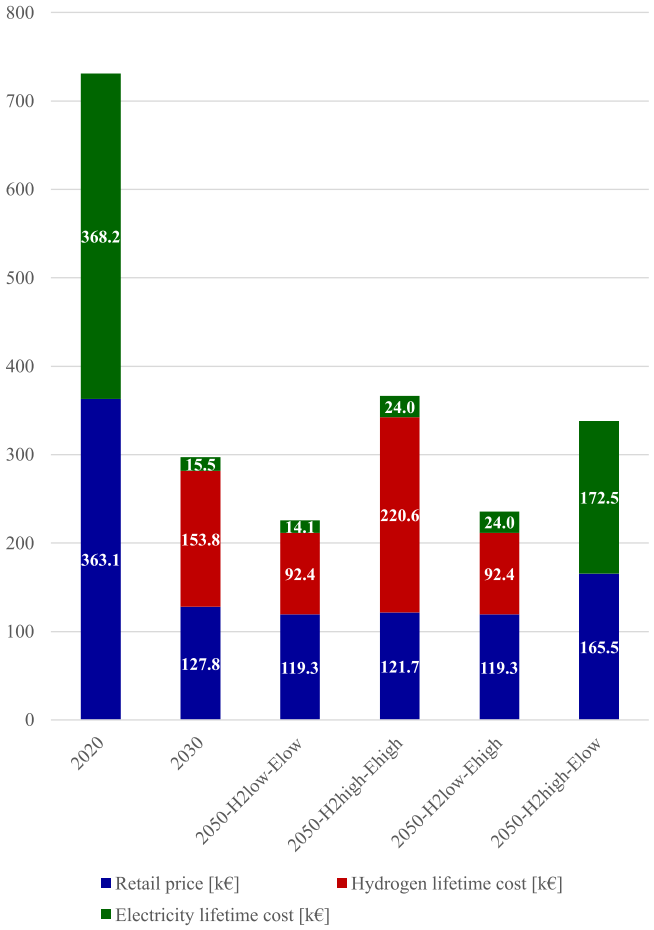

Fig. 5. Cost breakdown of suggested FCEV powertrain layouts across retained cost scenarios.

the forecasted electricity price for 2020, 2030 and 2050 oriented scenarios. 2020, 2030 and 2050 oriented scenarios differ in this case concerning the values of price parameters related to the development and manufacturing of fuel cell electrified truck components (i.e. α_{FC}, α_{ba}, α_{ba}). The set of values for these three coefficients is thus fixed in each year scenario, while the hydrogen price α_{H2} and the electricity price α_{elec} become the

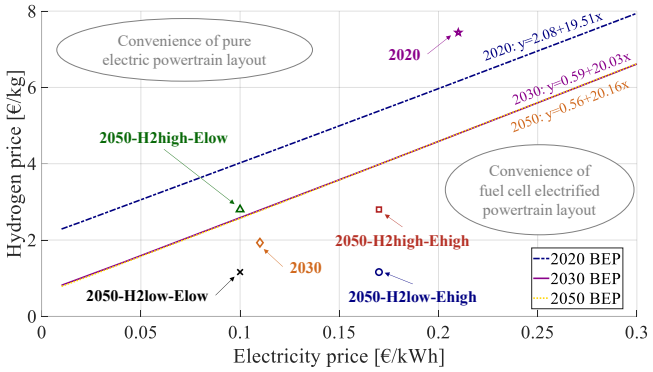

Fig. 6. Break-even lines between pure electric powertrain layout and fuel cell electrified powertrain layout for the considered heavy-duty truck in the retained cost scenarios as function of predicted electricity price and predicted hydrogen price.

two independent variables driving the TCO of the sizing options for the fuel cell electrified truck. Then, the FCEV sizing results obtained in the previous sub-section are explored while exhaustively sweeping different combinations of values for α_{H2} and α_{elec}. For a given year scenario, the break-even point in terms of α_{H2} value for a given value of α_{elec} relates to have at least one fuel cell electrified powertrain sizing candidate exhibiting lower TCO compared with the battery electric sizing powertrain sizing candidate. This leads to draw three break-even lines in Fig. 6 which respectively relate to 2020, 2030 and 2050 oriented scenarios. Obtained equations for break-even lines of 2020, 2030 and 2050 oriented scenario are reported in eq. (18), eq. (19) and eq. (20), respectively.

$$\alpha_{H2-bep-2020} = 2.08 + 19.51 \cdot \alpha_{elec} \quad (18)$$

$$\alpha_{H2-bep-2030} = 0.59 + 20.03 \cdot \alpha_{elec} \quad (19)$$

$$\alpha_{H2-bep-2050} = 0.56 + 20.16 \cdot \alpha_{elec} \quad (20)$$

$\alpha_{H2-bep-2020}$, $\alpha_{H2-bep-2030}$ and $\alpha_{H2-bep-2050}$ stand for hydrogen price targets in euro per kilogram which allow achieving equal TCO between a fuel cell electrified truck and a pure electric truck as a function of the electricity price in 2020, 2030 and 2050 oriented scenarios, respectively. For a given value of electricity price, economic attractiveness of a fuel cell electrified truck layout over a pure electric truck layout relates to the value of hydrogen price being lower than α_{H2-bep} for the corresponding year scenario.

Hydrogen prices for both "2020" and "2050-H2highElow" scenarios are located above the corresponding break-even lines in Fig. 6, which involve convenience of the pure electric powertrain layout. On the other hand, convenience of a fuel cell electrified powertrain layout is suggested in Fig. 6 for the heavy-duty truck in the remaining cost scenarios since they are located below the corresponding break-even lines. This kind of results may help designers and engineers in selecting the most appropriate heavy-duty truck powertrain layout as function of forecasted future electricity price and hydrogen price.

V. CONCLUSIONS

This paper aims at presenting a TCO-oriented sizing

methodology for fuel cell electrified heavy-duty trucks. The adopted numerical modelling procedure and optimal energy management strategy for a FCEV have been discussed first. The implemented cost-oriented powertrain sizing procedure has then been illustrated which involves evaluating the overall vehicle mass, assessing the hydrogen and electrical energy economy capabilities, and estimating the retail price and the TCO of each sizing candidate. The flexibility of the implemented sizing methodology has been demonstrated by considering six different present-oriented, 10-year oriented and 30-year oriented cost scenarios.

Obtained results suggest that, from a TCO perspective, a battery electric powertrain layout may currently be suggested outperforming a fuel cell electrified powertrain layout. This implication mainly stems from higher current cost factors for fuel cell system production, hydrogen storage system production and hydrogen refueling. Yet, this entails remarkable upsizing both the battery pack capacity and the overall vehicle weight. On the other hand, when rightsized following the proposed methodology, a fuel cell electrified powertrain option is suggested to be more appealing in a 10-year (i.e. 2030) oriented cost scenario, involving consistent reductions both in the truck weight, the battery pack capacity, and the retail price. As concerns 30-year (i.e. 2050) oriented cost scenarios, a fuel cell electrified powertrain layout is still suggested as more viable for the heavy-duty truck than a battery electric powertrain, except a decrease in the electricity price would be forecasted along with a considerable increase in the hydrogen price.

The presented methodology is generalized and can be applied to different heavy-duty truck parameters. Here, the validity of the predicted FCEV sizing results depends on the future cost trends being in line with current forecast. This requires future synergic advances in fuel cell propulsion technologies, in high-voltage battery technologies, in hydrogen production and refueling infrastructure, and in electricity production and charging infrastructure. Engineers may adopt the presented methodology at early vehicle design phases to appropriately size fuel cell electrified propulsion systems of long-haul heavy-duty trucks as function of actual or forecasted cost parameters.

Regarding FCEV energy management, implementing the retained DP based global optimal control approach on-board fuel cell electrified trucks may currently be difficult due to the significant computational cost involved and the requirement of a priori knowledge of future driving conditions over an extended time horizon (e.g. several minutes). However, the optimal control trajectories identified by DP can pave the way for developing enhanced real-time capable energy management approaches [60]. For instance, DP can be used to set appropriately the targets and to benchmark the performance of real-time FCEV energy management strategies and consequently fine-tune them. A related example is provided in [61], where a Pontryagins's Minimum Principle based FCEV energy management was demonstrated achieving only 1.5% higher hydrogen consumption compared with the optimal benchmark provided by DP. Moreover, in [62] control results obtained using DP were analyzed to improve the calibration of an adaptive rule-based control strategy for a fuel cell hybrid railway vehicle. Also in this case, fine tuning the real-time rule-based control approach led to limit the increase in hydrogen consumption within only 1.3% compared with the DP optimal off-line reference.

Related future work may involve increasing the FCEV model fidelity level (e.g. considering greenhouse gases as in [63], or fuel cell system temperature as in [64][65], or fuel cell system degradation as in [66][67]), and in turn the complexity of the energy management problem. Moreover, different fuel cell types, battery chemistries, driving missions and truck loading conditions may be assessed as example. Finally, the computational efficiency of the proposed methodology may be enhanced by implementing different optimization-based sizing space exploration algorithms.

ACKNOWLEDGEMENTS

This research work was promoted by the Interdepartmental Center for Automotive Research and Sustainable Mobility (CARS) at Politecnico di Torino (www.cars.polito.it).

REFERENCES

[1] B. Bilgin *et al*., "Making the Case for Electrified Transportation," in *IEEE Transactions on Transportation Electrification*, vol. 1, no. 1, pp. 4-17, June 2015.

[2] B. Cox, C. Bauer, A.M. Beltran, D.P. van Vuuren, C.L. Mutel, "Life cycle environmental and cost comparison of current and future passenger cars under different energy scenarios", *Applied Energy*, vol. 269, no. 115021, 2020.

[3] I. Aghabali, J. Bauman, P. Kollmeyer, Y. Wang, B. Bilgin and A. Emadi, "800V Electric Vehicle Powertrains: Review and Analysis of Benefits, Challenges, and Future Trends," in *IEEE Transactions on Transportation Electrification*, vol. 7, no. 3, 2021.

[4] X. Liu, C. B. Soh, S. Yao, H. Zhang and T. Zhao, "Operation Management of Multiregion Battery Swapping–Charging Networks for Electrified Public Transportation Systems," in *IEEE Transactions on Transportation Electrification*, vol. 6, no. 3, pp. 1013-1025, Sept. 2020.

[5] Z. Bi, T. Kan, C.C. Mi, Y. Zhang, Z. Zhao and G.A. Keoleian, "A review of wireless power transfer for electric vehicles: Prospects to enhance sustainable mobility", *Applied Energy*, vol. 179, pp. 413-425, 2016.

[6] P. Venugopal, A. Shekhar, E. Visser, N. Scheele, G.R.C. Mouli, P. Bauer and S. Silvester, "Roadway to self-healing highways with integrated wireless electric vehicle charging and sustainable energy harvesting technologies", *Applied energy*, vol. 212, pp. 1226-1239, 2018.

[7] K. Forrest, M. Mac Kinnon, B. Tarroja, S. Samuelsen, "Estimating the technical feasibility of fuel cell and battery electric vehicles for the medium and heavy duty sectors in California", *Applied Energy*, vol. 276, no. 115439, 2020.

[8] J. Kast, R. Vijayagopal, J.J. Gangloff Jr, J. Marcinkoski, "Clean commercial transportation: Medium and heavy duty fuel cell electric trucks", *International Journal of Hydrogen Energy*, vol. *42*, no. 7, pp. 4508-4517, 2017.

[9] Y. Wang, H. Yuan, A. Martinez, P. Hong, H. Xu and F.R. Bockmiller, "Polymer Electrolyte Membrane Fuel Cell and Hydrogen Station Network for Automobiles: Status, Technology, and Perspectives", *Advances in Applied Energy*, vol. 100011, 2021.

[10] F. Grüger, L. Dylewski, M. Robinius and D. Stolten, "Carsharing with fuel cell vehicles: Sizing hydrogen refueling stations based on refueling behavior", *Applied energy*, vol. 228, pp. 1540-1549, 2018.

[11] M. Schröder, Z. Abdin and W. Mérida, “Optimization of distributed energy resources for electric vehicle charging and fuel cell vehicle refueling”, *Applied Energy*, vol. *277*, pp. 115562, 2020.

[12] H. Oh, W.Y. Lee, J. Won, M. Kim, Y.Y. Choi and S.B. Han, “Residual-based fault diagnosis for thermal management systems of proton exchange membrane fuel cells”, *Applied Energy*, vol. 277, no. 115568, 2020.

[13] Y. Akimoto and K. Okajima, “Simple on-board fault-detection method for proton exchange membrane fuel cell stacks using by semi-empirical curve fitting”, *Applied Energy*, vol. 303, no. 117654, 2021.

[14] Y. Wu and H. Gao, "Optimization of Fuel Cell and Supercapacitor for Fuel-Cell Electric Vehicles," in *IEEE Transactions on Vehicular Technology*, vol. 55, no. 6, pp. 1748-1755, Nov. 2006.

[15] O. Hegazy and J. Van Mierlo, "Particle Swarm Optimization for optimal powertrain component sizing and design of fuel cell hybrid electric vehicle," *2010 12th International Conference on Optimization of Electrical and Electronic Equipment*, 2010, pp. 601-609.

[16] D. Feroldi and M. Carignano, “Sizing for fuel cell/supercapacitor hybrid vehicles based on stochastic driving cycles”, *Applied energy*, vol. 183, pp. 645-658, 2016.

[17] L. Xu, M. Ouyang, J. Li, F. Yang, L. Lu and J. Hua, “Optimal sizing of plug-in fuel cell electric vehicles using models of vehicle performance and system cost”, *Applied Energy*, vol. 103, pp. 477-487, 2013.

[18] M. Jain, C. Desai and S. S. Williamson, "Genetic algorithm based optimal powertrain component sizing and control strategy design for a fuel cell hybrid electric bus," *2009 IEEE Vehicle Power and Propulsion Conference*, 2009, pp. 980-985.

[19] J. Bauman and M. Kazerani, "A Comparative Study of Fuel-Cell–Battery, Fuel-Cell–Ultracapacitor, and Fuel-Cell–Battery–Ultracapacitor Vehicles," in *IEEE Transactions on Vehicular Technology*, vol. 57, no. 2, pp. 760-769, March 2008.

[20] J. Bernard, S. Delprat, F. N. Buchi and T. M. Guerra, "Fuel-Cell Hybrid Powertrain: Toward Minimization of Hydrogen Consumption," in *IEEE Transactions on Vehicular Technology*, vol. 58, no. 7, pp. 3168-3176, Sept. 2009.

[21] N. Lutsey, C.J. Brodrick, T. Lipman, “ Analysis of potential fuel consumption and emissions reductions from fuel cell auxiliary power units (APUs) in long-haul trucks”, *Energy*, vol. *32*, no. 12, pp. 2428-2438, 2007.

[22] K. Sim, R. Vijayagopal, N. Kim, A. Rousseau, “Optimization of Component Sizing for a Fuel Cell-Powered Truck to Minimize Ownership Cost”, *Energies*, vol. 12, no. 6, pp. 1125, 2019.

[23] T. Jokela, A. Iraklis, B. Kim, B. Gao, “Combined Sizing and EMS Optimization of Fuel-Cell Hybrid Powertrains for Commercial Vehicles,” *SAE Technical Paper* 2019-01-0387, 2019.

[24] C. Wen, B. Rogie, M.R. Kærn and E. Rothuizen, “A first study of the potential of integrating an ejector in hydrogen fuelling stations for fuelling high pressure hydrogen vehicles”, *Applied Energy*, vol. *260*, no. 113958, 2020.

[25] J. Kast, G. Morrison, J.J. Gangloff Jr, R. Vijayagopal, J. Marcinkoski, “Designing hydrogen fuel cell electric trucks in a diverse medium and heavy duty market”, *Research in Transportation Economics*, vol. 70, pp. 139-147, 2018.

[26] G. Rizzoni, L. Guzzella and B. M. Baumann, "Unified modeling of hybrid electric vehicle drivetrains," in *IEEE/ASME Transactions on Mechatronics*, vol. 4, no. 3, pp. 246-257, Sept. 1999.

[27] F.J.R. Verbruggen, E. Silvas, T. Hofman, “Electric Powertrain Topology Analysis and Design for Heavy-Duty Trucks”, *Energies*, vol. 13, no. 10:2434, 2020.

[28] F. Berr, A. Abdelli, D. Postariu, R. Benlamine, “Design and Optimization of Future Hybrid and Electric Propulsion Systems: An Advanced Tool Integrated in a Complete Workflow to Study Electric Devices.” *Oil & Gas Science and Technology*, vol. 67, pp. 547-562, 2012.

[29] S.G. Lias et al., "Ion Energetics Data in NIST Chemistry WebBook, NIST Standard Reference Database Number 69," *National Institute of Standards and Technology, Gaithersburg MD* 20899, 2018.

[30] S. Molina, R. Novella, B. Pla and M. Lopez-Juarez, “Optimization and sizing of a fuel cell range extender vehicle for passenger car applications in driving cycle conditions”, *Applied Energy*, vol. 285, no. 116469, 2021.

[31] P.G. Anselma, G. Belingardi, “Multi-objective optimal computer-aided engineering of hydraulic brake systems for electrified road vehicles”, *Vehicle System Dynamics*, in press, 2021.

[32] Y. Guezennec, Ta-Young Choi, G. Paganelli and G. Rizzoni, "Supervisory control of fuel cell vehicles and its link to overall system efficiency and low-level control requirements," *Proceedings of the 2003 American Control Conference, 2003.*, 2003, pp. 2055-2061 vol.3.

[33] M. Kandidayeni, A. Macias, L. Boulon, S. Kelouwanic, “Investigating the impact of ageing and thermal management of a fuel cell system on energy management strategies”, *Applied Energy*, vol. 274, no. 115293, 2020.

[34] R. Bellman and E. Lee, "History and development of dynamic programming," in *IEEE Control Systems Magazine*, vol. 4, no. 4, pp. 24-28, November 1984.

[35] L. Xu, C.D. Mueller, J. Li, M. Ouyang and Z. Hu, “Multi-objective component sizing based on optimal energy management strategy of fuel cell electric vehicles”, *Applied energy*, 157, 664-674, 2015.

[36] T. Hofman, S. Ebbesen and L. Guzzella, "Topology Optimization for Hybrid Electric Vehicles With Automated Transmissions," in *IEEE Transactions on Vehicular Technology*, vol. 61, no. 6, pp. 2442-2451, July 2012.

[37] S. Ebbesen, C. Donitz, L. Guzzella, "Particle swarm optimisation for hybrid electric drive-train sizing", *Int. J. Vehicle Design*, Vol. 58, Nos. 2/3/4, 2012.

[38] Y. Sun, S. Li, X. Fu, W. Dong, M. Ramezani and B. Balasubramanian, "Approximate Dynamic Programming Vector Controllers for Operation of IPM Motors in Linear and Overmodulation Regions," in *IEEE Transactions on Transportation Electrification*, vol. 7, no. 2, pp. 659-670, June 2021.

[39] H. Zhu, Z. Song, J. Hou, H. F. Hofmann and J. Sun, "Simultaneous Identification and Control Using Active Signal Injection for Series Hybrid Electric Vehicles Based on Dynamic Programming," in *IEEE Transactions on Transportation Electrification*, vol. 6, no. 1, pp. 298-307, March 2020.

[40] O. Sundstrom and L. Guzzella, "A generic dynamic programming Matlab function," *2009 IEEE Control Applications, (CCA) & Intelligent Control, (ISIC)*, 2009, pp. 1625-1630.

[41] P. Elbert, S. Ebbesen and L. Guzzella, "Implementation of Dynamic Programming for n-Dimensional Optimal Control Problems With Final State Constraints," in *IEEE Transactions on Control Systems Technology*, vol. 21, no. 3, pp. 924-931, May 2013.

[42] Y. Zhou, A. Ravey, M.C. Péra, “Multi-mode predictive energy management for fuel cell hybrid electric vehicles using Markov driving pattern recognizer”, *Applied Energy*, vol. 258, no. 114057, 2020.

[43] M. Iqbal, M. Becherif, H.S. Ramadan and A. Badji, “Dual-layer approach for systematic sizing and online energy management of fuel cell hybrid vehicles”, *Applied Energy*, vol. 300, no. 117345, 2021.

[44] Y. Kim, M. Figueroa-Santos, N. Prakash, S. Baek, J.B. Siegel and D. M. Rizzo, “Co-optimization of speed trajectory and power management for a fuel-cell/battery electric vehicle. *Applied Energy*, vol. 260, no. 114254, 2020.

[45] N. Sulaiman, M.A. Hannan, A. Mohamed, P.J. Ker, E.H. Majlan, W.W. Daud, “ Optimization of energy management system for fuel-cell hybrid electric vehicles: Issues and recommendations”, *Applied energy*, vol. 228, pp. 2061-2079, 2018.

[46] Hyundai Truck & Bus, “Hyundai Motor Upgrades Design and Performance of XCIENT Fuel Cell Truck for Global

Expansion", [online] available: https://www.hyundai.com/worldwide/en/company/newsroom/hyundai-motor-upgrades-design-and-performance-of-xcient-fuel-cell-truck-for-global-expansion-0000016662 (accessed 7 Jul. 2021).

[47] E. Rivard, M. Trudeau, K. Zaghib, "Hydrogen Storage for Mobility: A Review", *Materials*, vol. 12, no. 12, pp. 1973, 2019.

[48] K. B. Wipke, M. R. Cuddy and S. D. Burch, "ADVISOR 2.1: a user-friendly advanced powertrain simulation using a combined backward/forward approach," in *IEEE Transactions on Vehicular Technology*, vol. 48, no. 6, pp. 1751-1761, Nov. 1999.

[49] H. Liimatainen, O. Van Vliet, D. Aplyn, "The potential of electric trucks–An international commodity-level analysis", *Applied Energy*, vol. 236, pp. 804-814, 2019.

[50] C. Navas, "Development of Business Cases for Fuel Cells and Hydrogen Applications for Regions and Cities - FCH Heavy-duty trucks", [online] available: https://www.fch.europa.eu/sites/default/files/171121_FCH2JU_Application-Package_WG1_Heavy%20duty%20trucks%20%28ID%202910560%29%20%28ID%202911646%29.pdf (accessed 8 Jul. 2021).

[51] Battelle Memorial Institute, "Manufacturing Cost Analysis of 100 and 250 kW Fuel Cell Systems for Primary Power and Combined Heat and Power Applications", *U.S. Department of Energy*, 2016.

[52] E. Taibi et al., "Hydrogen from renewable power: technology outlook for the energy transition", International Renewable Energy Agency: Abu Dhabi, UAE, 2018.

[53] G. Parks et al., "Hydrogen Station Compression, Storage, and Dispensing Technical Status and Costs", Technical Report of the National Renewable Energy Laboratory, 2014.

[54] Eurostat, "Electricity prices by type of user", [online] available: https://ec.europa.eu/eurostat/databrowser/view/ten00117/default/table?lang=en (accessed 8 Jul. 2020).

[55] A. Nase, K. Kruger, "Hydrogen Society Impact on Transport Sector", *FEV Online Seminar*, March 2021.

[56] Institute for Energy Economics and Financial Analysis, "Green hydrogen to be cost-competitive by 2030—BloombergNEF", [online] available: https://ieefa.org/green-hydrogen-to-be-cost-competitive-by-2030-bloombergnef/ (accessed 13 Jul. 2021).

[57] P. Capros, A. De Vita, N. Tasios, et al., "EU Energy, Transport and GHG Emissions, Trends to 2050: Reference Scenario 2013", *European Commission*, 2013.

[58] A. Christensen, "Assessment of Hydrogen Production Costs from Electrolysis: United States and Europe", *International Council on Clean Transportation: Washington, DC, USA*, 2020.

[59] E. Taibi, H. Bianco, R. Miranda, M. Carmo, "Green hydrogen cost reduction - Scaling up electrolysers to meet the 1.5°C climate goal", *International Renewable Energy Agency*, 2020.

[60] Anselma P.G., "Computationally efficient evaluation of fuel and electrical energy economy of plug-in hybrid electric vehicles with smooth driving constraints", *Applied Energy*, 307, 118247, 2022.

[61] Peng H., Chen Z., Li J., Deng K., Dirkes S., Gottschalk J., Unlubayir C. et al., "Offline optimal energy management strategies considering high dynamics in batteries and constraints on fuel cell system power rate: From analytical derivation to validation on test bench", *Applied Energy*, *282*, 116152, 2021.

[62] Peng, H., Li, J., Thul, A., Deng, K., Ünlübayir, C., Löwenstein, L., and Hameyer, K. "A scalable, causal, adaptive rule-based energy management for fuel cell hybrid railway vehicles learned from results of dynamic programming", *ETransportation*, *4*, 100057, 2020.

[63] J.M. Desantes, R. Novella, B. Pla and M. Lopez-Juarez, "Impact of fuel cell range extender powertrain design on greenhouse gases and NOX emissions in automotive applications", *Applied Energy*, vol. *302*, no. 117526, 2021.

[64] Z. Song, Y. Pan, H. Chen, and T. Zhang, "Effects of temperature on the performance of fuel cell hybrid electric vehicles: A review", *Applied Energy*, vol. 302, no. 117572, 2021.

[65] Z. Zeng, Y. Qian, Y. Zhang, C. Hao, D. Dan, and W. Zhuge, "A review of heat transfer and thermal management methods for temperature gradient reduction in solid oxide fuel cell (SOFC) stacks", *Applied Energy*, vol. 280, no. 115899, 2020.

[66] K. Song, Y. Ding, X. Hu, H. Xu, Y. Wang and J. Cao, J. "Degradation adaptive energy management strategy using fuel cell state-of-health for fuel economy improvement of hybrid electric vehicle", *Applied Energy*, vol. 285, no. 116413, 2021.

[67] Y. He, Y. Zhou, Z. Wang, J. Liu, Z. Liu, and G. Zhang, "Quantification on fuel cell degradation and techno-economic analysis of a hydrogen-based grid-interactive residential energy sharing network with fuel-cell-powered vehicles", *Applied Energy*, vol. 303, no. 117444, 2021.